



EFFECT OF COOLING MODE AFTER DIFFUSION WELDING AND BRAZING ON RESIDUAL STRESSES IN GRAPHITE–COPPER EDGE JOINTS

V.V. KVASNITSKY¹, G.V. ERMOLAEV² and M.V. MATVIENKO³

¹NTUU «Kiev Polytechnic Institute»

37 Pobeda Ave., 03056, Kiev, Ukraine. E-mail: kvas69@ukr.net

²National Shipbuilding University

9 Geroiv Staliningrada Ave., 54025, Nikolaev, Ukraine. E-mail: welding@nuos.edu.ua

³Kherson Branch of National Shipbuilding University

44 Ushakov Ave., 73022, Kherson, Ukraine. E-mail: matvienkomv@i.ua

Studied is stress-strain state at different modes of cooling of cylindrical assemblies from graphite and copper in plastic and elastic stages considering short-term plastic deformations as well as creep. Effect of cooling mode on plastic deformations in butt zone and axial stresses on assemblies' surface, determining possibility of fracture of brittle graphite was found. 7 Ref., 3 Tables, 12 Figures.

Keywords: *diffusion welding, brazing, graphite–copper joint, stress-strain state, cooling modes, residual stresses, mathematical modeling*

Graphite products are used in combination with many metals in current equipment. Graphite having high electric and heat conduction is widely used in development of current-carrying or current-collecting devices of different assemblies and machines, graphitized electrodes, sealing arrangements etc., where joining with metals is necessary. Brazing and diffusion welding [1, 2] are used for that. The general problem for both methods of joining are residual stresses caused by different thermal coefficients of linear expansion (TCLE) of materials to be joined. Residual stresses in ductile materials being joined usually result in degradation of shape and size, and can promote crack formation and fracture in graphite, which is a brittle material.

Metals with close to graphite TCLE are selected for reduction of stresses in metal-graphite assemblies. Many assemblies use titanium, which is not equal to graphite on electric and heat conduction. The best choice for indicated devices is copper, but it has significantly larger TCLE than graphite, that often results in crack formation in graphite after assembly cooling.

Our earlier researches [3, 4] were dedicated to investigation of dependencies of formation of stress and deformation fields in the butt zone in diffusion welding (DW) and brazing of parts from dissimilar materials. This information is necessary for updating assembly structure and production of quality joint. Some general de-

pendencies of formation of residual stresses were received for metal–ceramics joints in bush-to-bush joint assemblies, in which Young's modules of joined materials are equal [5]. But they are an order different in graphite and copper, that can have significant effect on stress-strain state (SSS) of the assembly in their joining. Therefore, investigation of SSS formation in copper-non-metallic assemblies is a relevant task.

Researches of graphite (ceramics)-to-metals joints showed that fracture is initiated by cracks appearing in the butt in non-metallic part [1]. Metal surface after complete fracture includes thin graphite layer as shown in Figure 1.

Aim of the investigation is study of peculiarities of SSS formation in cooling after DW and brazing of metal-graphite assemblies and effect of graphite and copper joining technology on it by computer modeling.

Investigations were carried out by computer modeling method using license software complex ANSYS (vers. 10). Axially symmetric problems



Figure 1. Fracture surface of metal (1) to graphite (2) joint

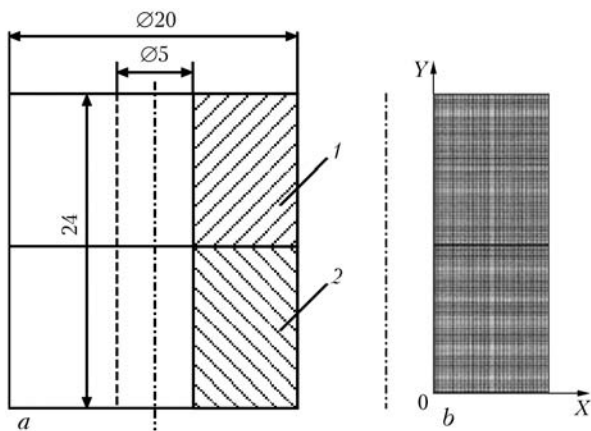


Figure 2. View of B-B assembly (a) and its finite element model (b): 1 – copper bush; 2 – graphite bush

with finite elements of PLANE 182 type were solved.

Edge joints, which are usually used in current-carrying devices, were taken for investigations. Modeling was carried out for bush-to-bush (B-B) assembly. This model in comparison with bar or cylinder is more informative since has two-side surfaces and being easily transformed in cylinder with inner radius equal zero, and rules of SSS formation in cylinder-cylinder type assemblies are also preserved for bar-bar type assemblies as shown in works [6, 7].

View of B-B assembly and section of its finite element model are shown in Figure 2. This model can be used for joints made by pressure brazing, eliminating brazing metal interlayer due to its small thickness.

Table 1 shows thermal-physical properties of copper and graphite, taken in calculations.

Assembly cooling in 900 to 500 °C range, in which creep resistance has a significant effect on stress relief, was considered for investigation of general dependencies of SSS formation.

Table 1. Thermal-physical properties of materials joined

Material	Temperature, °C	Young's modulus $E \cdot 10^3$, MPa	Poisson's coefficient	TCLE · 10 ⁶ , 1/deg	Yield strength, MPa	Strengthening modulus · 10 ³ , MPa
Graphite	20	9.3	0.18	4.8	–	–
	200	9.4		5.0	–	–
	400	9.8		5.1	–	–
	700	10.3		5.5	–	–
	900	10.8		5.7	–	–
Copper	20	125	0.34	16.7	69	1.5
	200	110		17.2	60	1.3
	400	100		17.8	45	0.9
	700	60		19.4	17.3	0.8
	800	40		20.5	11.5	0.7
	900	38		19.8	8.5	0.6

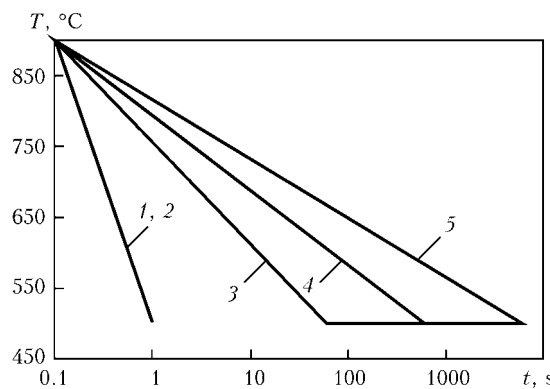


Figure 3. Thermal cycles of cooling for studied five variants (1–5)

Modeling was carried out for 5 variants of temperature reduction in indicated interval:

- elastic solution at temperature reduction to 500 °C (variant 1);
- elastic-plastic solution at quick reduction of temperature to 500 °C (variant 2), where creep deformations are negligibly small;
- elastic-plastic solution considering creep at gradual reduction of temperature to 500 °C in course of 60 s and further holding during 6000 s at 500 °C (variant 3);
- elastic-plastic solution considering creep at gradual reduction of temperature to 500 °C during 600 s and further holding at 500 °C up to 6000 s (variant 4);
- elastic-plastic solution considering creep at gradual reduction of temperature to 500 °C during 6000 s (variant 5).

Figure 3 provides for thermal cycles for considered variants.

Copper creep rate in variants 3–5 was determined by equation

$$\dot{\epsilon} = C_1 \sigma^{C_2} e^{\frac{C_3}{T}}$$

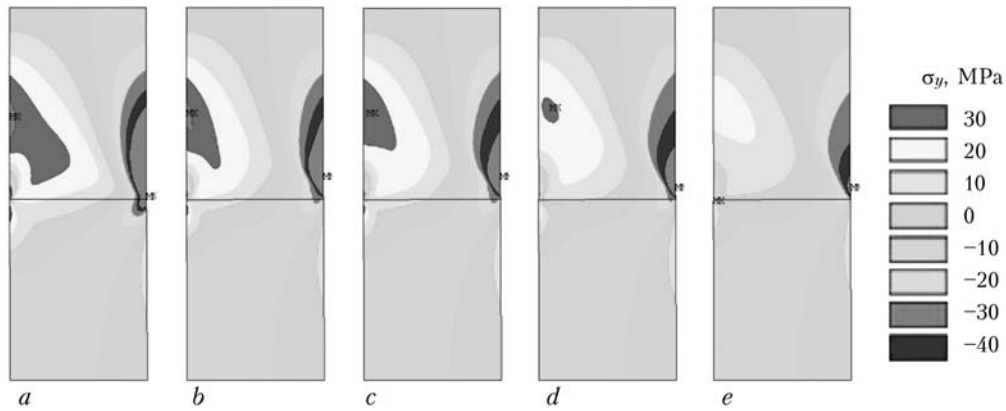


Figure 4. Axial stresses after cooling to 500 °C in variants 1 (a), 2 (b), 3 (c), 4 (d) and 5 (e)

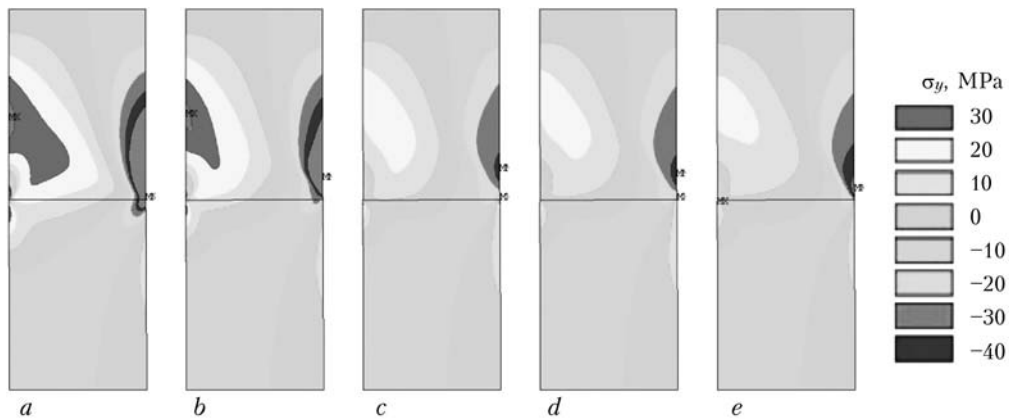


Figure 5. Axial stresses after cooling and holding in variants 1 (a), 2 (b), 3 (c), 4 (d) and 5 (e)

where $C_1 = 1.67 \cdot 10^{-30}$, $C_2 = 5$, $C_3 = 25872$ are the equation coefficients, received by us experimentally in investigation of copper creep.

Fields and diagrams of distribution of stresses, deformations and movements at different stages of cooling, including the moments of end of temperature reduction (all variants) and end of holding at 500 °C (variants 3 and 4), were analyzed. Further only fields and diagrams of axial stresses are given. They, as shown in work [5], are the main reason of brittle fracture of materials with low TCLE.

Analysis of stress fields for different cooling variants showed that all stress constituents, including equivalent ones, significantly change at cooling rate variation, in particular in copper

(Figure 4). Further holding at 500 °C (variants 3 and 4) promotes more changes in them (Figure 5). At that radial, circumferential, tangential and equivalent stresses are concentrated close to the butt, and axial stresses are in internal and external surfaces of the bush.

Plastic deformation are distributed in accordance to stresses, i.e. from copper side in the vicinity to the butt, to the most extent at distance of around 1/4 of bush thickness from its external surface (Figures 6 and 7).

Analysis of fields and values of plastic deformations (Table 2) showed that instantaneous deformations in copper reduce from 1.4 % in variant 1 to zero in variant 5 with increase of cooling time. Creep deformations at temperature reduc-

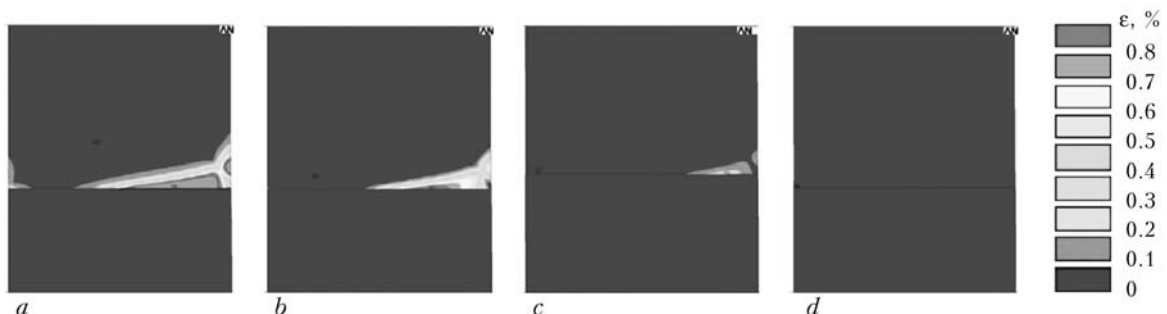


Figure 6. Equivalent deformations of instantaneous plasticity after cooling to 500 °C in variants 2 (a), 3 (b), 4 (c) and 5 (d)

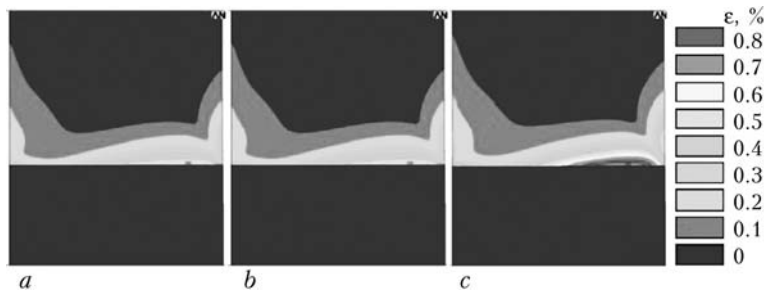


Figure 7. Equivalent creep deformations after cooling and holding in variants 3 (a), 4 (b) and 5 (c)

tion stage, on the contrary, significantly increase with rise of cooling time to 500 °C (from 0.4 % in variant 3 to 1.05 % in variant 5). Total plastic deformations at cooling stage reduce from 1.4 % in variant 2 to 1.05 % in variant 5.

Creep deformations show insignificant rise (0.19 and 0.22 %) in process of holding at constant temperature 500 °C (variants 3 and 4). As a result, total creep deformations for the whole period of cooling and holding at 500 °C increase with rise of cooling time and corresponding decrease of time of holding from 0 (variant 2) to 1.05 % (variant 5), whereas sum ones (instantaneous and plastic) reduce from 1.4 % (variant 2) to 1.05 % (variant 5).

Thus, increase of cooling rate is more efficient than increase of time of holding after temperature decrease from the point of view of development of short-term plastic deformations in copper. And, vice versa, slow cooling is more efficient from the point of creep deformations.

Nature of fields of short-term and creep plastic deformations are also distinguished (Figures 6 and 7). The short-term deformations are mostly concentrated close to the butt in its part adjacent to the external surface (Figure 6). The creep deformations cover all butt area at distance comparable with bush thickness (Figure 7). At that, they significantly reduce (Figures 6, b and 7, a) in process of long-term holding at 500 °C (variant 3).

Effect of plastic deformations in copper on axial stresses appearing on graphite side surface is caused by two mechanisms. On the one hand, in accordance with the general principles of mechanics, plastic deformation of copper provides for reduction of level of stresses in it and, respectively, preserve assembly equilibrium conditions in graphite. On the other hand, they effect bend shape of generatrix, which also influences the level and nature of stress distribution in copper [5]. Nature of this effect is ambiguous. Plastic deformations in copper can increase as well as reduce surface curvature, respectively increasing or reducing stress level.

Elastic and plastic deformation of bush material result in change of its surface shape. Analysis of diagrams of radial movements of points of external surface showed (Figure 8) that the nature of generatrix bending is almost kept the same, as at equal rigidity of materials being joined [5]. However, their skew-symmetries relatively to butt plane at elastic loading (variant 1) are significantly violated. The generatrix from the side

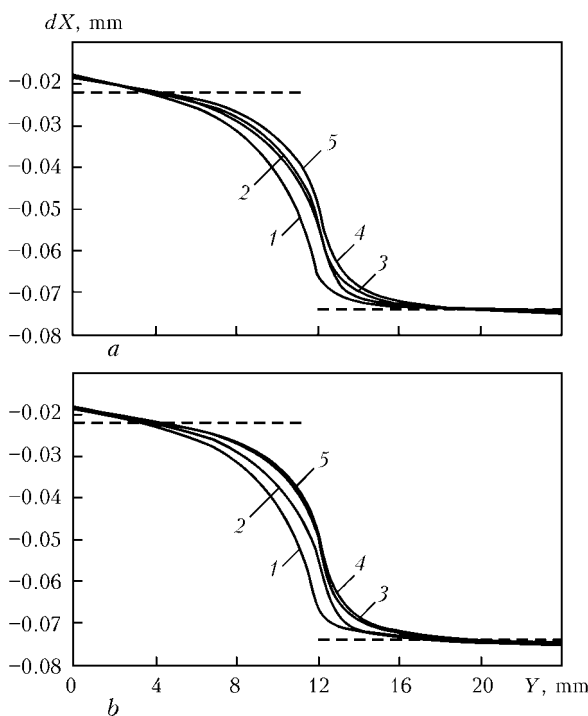


Figure 8. Diagrams of radial movements of points of bush external surface after cooling to 500 °C (a) and after cooling and holding (b) for variants 1–5 (1–5)

Table 2. Maximum plastic (equivalent) deformations in copper, %

Variant	End of cooling			End of holding	Sum
	Instantaneous deformations	Creep deformations	Sum	Creep deformations	
2	1.40	0	1.40	0	1.40
3	0.90	0.40	1.30	0.59	1.49
4	0.23	0.75	0.98	0.97	1.21
5	0	1.05	1.05	1.05	1.05



of more rigid material (copper) shows less bending, approaching to free contraction state (see dashed line in Figure 8). The situation is opposite and the bend is significantly increased from the side of less rigid material (graphite).

Bend in more rigid, but ductile material (copper) increases and that in less rigid elastic material (graphite) reduces, shape of bend of the generatrix approaches to symmetric one in appearance of plastic instantaneous and creep deformations (variants 2–5). In other words, the short-term plastic deformations, developing at quick cooling, and creep deformations (variants 3–5) compensate higher rigidity of copper in elastic state in comparison with graphite and equalize deformations of external surface in the butt region.

At that, the diagrams of radial movements of points of external surface after cooling and holding are virtually matched in variants 3–5 regardless some differences in value of maximum plastic deformations in copper (see Table 2).

Nature of radial movement of the points of internal side surface is more complex (Figure 9). A convex part of the graphite surface (material with lower TCLE) in immediate proximity to the butt (1–2 mm) gradually passes into a concave one with the removal from it. The situation is different in copper (material with larger TCLE), in which concave surface close to the butt gradually passes into a convex one with the removal from it.

Such a complex bend shape of the generatrix on internal surface of the bush is explained in work [5] by oncoming effect of two factors. On the one hand, this is a difference of mutual shift of upper and lower parts of the bush due to different change of their diameters, and, on the other hand, it is various change of section width at temperature contraction of materials of upper (metal) and lower (graphite) parts of the assembly.

Mutual shift of upper and lower parts of the bushes results in formation of convexity on the external and concavity on the internal surface of material with lower TCLE (graphite). Different change of width results in formation of convexity on the both sides of this material. As a consequence of simultaneous effect of both factors a nature of bend of the external surface, i.e. outside convexity, is preserved and the internal one being significantly changed.

Presence (effect) of two mechanisms of movement is also verified by absence of symmetry of the fields of plastic deformations and diagrams of tangential stresses relatively to middle of the bush thickness. Quantitative characteristic of effect of shift of the bush parts can be a level of

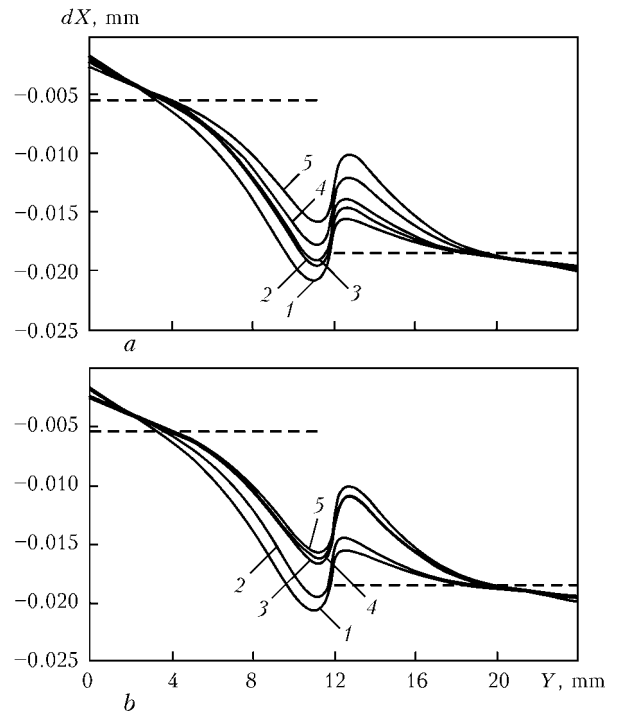


Figure 9. Diagrams of radial movements of points of bush internal surface after cooling to 500 °C (a) and after complete cooling and holding (b) for variants 1–5 (1–5)

tangential stresses in the middle of bush thickness (around 20 MPa).

Nature of bend of the internal surface is preserved at change of cooling rate, but value of movement is reduced at decrease of cooling rate (variants 3–5). Difference in movements is reduced at further holding (see Figure 9).

Axial stresses are distributed in accordance with surface deformation (Figures 10 and 11). They are compressive on the external surface in upper copper bush (with larger TCLE) and tensile ones in graphite lower part (with lower TCLE) (see Figures 4, 5 and 10).

After cooling tensile stresses for all variants reach maximum value (around 14 MPa) close to the butt (at 2–3 mm distance), and show gradual 2 times reduction at approaching to it (Figure 10, a). Further holding at 500 °C in variants 3 and 4, when creep deformations are added to short-term deformations, results in the fact that maximum stresses in graphite near the butt, on the contrary, rapidly increase to 30–35 MPa (Figure 10, b) and maximum point is right up to the butt.

The distribution is much more complex (see Figure 11) on the internal surface. Axial stresses in the lower graphite bush are of the tensile nature, they reduce to the zero step-by-step (at 2–3 mm distance from the butt) and transform in the compressive ones at removal from the joint, and then they again reduce to the zero at the edge.

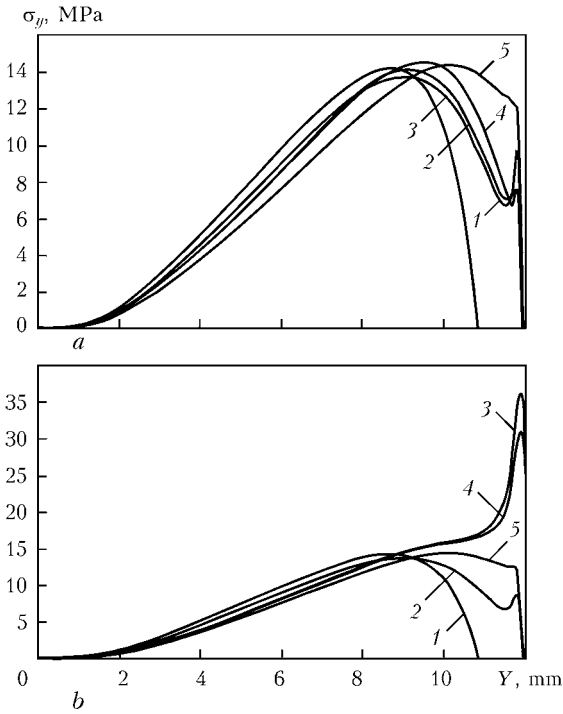


Figure 10. Diagrams of axial stresses on external surface of graphite after cooling (a) and after cooling and holding at 500 °C (b) for models 1–5 (1–5)

Table 3 and Figure 12 for convenience of comparison of the variants provide for the values and diagrams of maximum tensile stresses in graphite after cooling to 500 °C and holding at this temperature during 6000 s.

Analysis of the Table and Figures show that the internal surface is exposed to the most danger

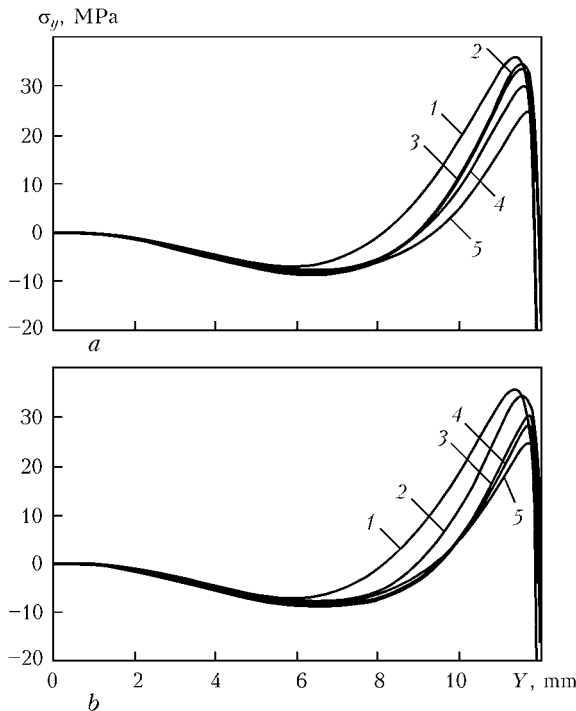


Figure 11. Diagrams of axial stresses on internal surface of graphite after cooling (a) and after cooling and holding at 500 °C (b) for models 1–5 (1–5)

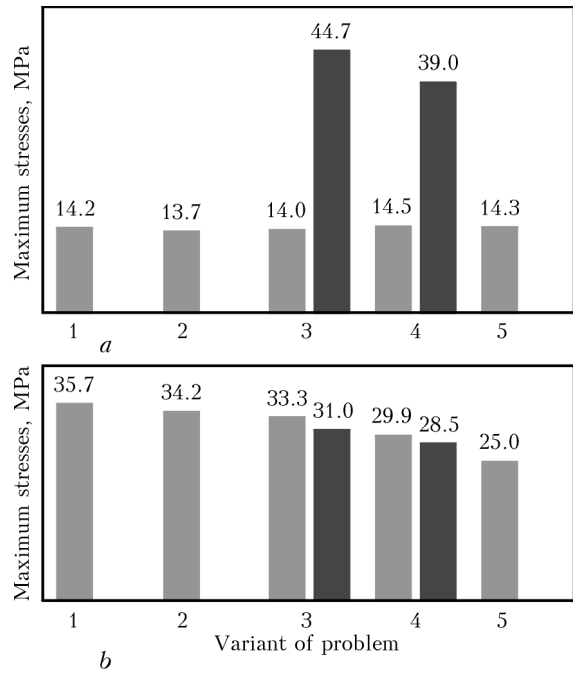


Figure 12. Maximum tensile stresses on external (a) and internal (b) surfaces of graphite in variants 1–5 after cooling to 500 °C and holding at this temperature (variants 3 and 4)

from the point of view of crack formation in graphite after cooling. At that, for all variants except for variant 5, the maximum tensile stresses reach bending strength of graphite (45 MPa for MPG-8 graphite and 34.3 MPa for MPG-6 and MPG-7 graphite). Variants 3 and 4 are dangerous for the external surface. Using them holding after cooling will result in larger tensile stresses.

Thus, the optimum, from the point of view of reduction of danger of crack formation in graphite after cooling to 500 °C, shall be variant 5 (gradual reduction of temperature from 900 to 500 °C during 6000 s) at which tensile stresses do not exceed 25 MPa.

Variants with quick cooling and further holding are not reasonable, since large stresses are developed on the external surface of graphite at them.

Further cooling of the assembly to 20 °C takes place under conditions of growth of yield point

Table 3. Maximum tensile stresses in graphite, MPa

Variant	On external surface		On internal surface	
	End of cooling	End of holding	End of cooling	End of holding
1	14.2	–	35.7	–
2	13.7	–	34.2	–
3	14.0	44.7	33.3	31.0
4	14.5	39.0	29.9	28.5
5	14.3	14.3	25.0	25.0



and creep resistance. Creep rate reduces and residual stresses exceed graphite strength limit (more than 65 MPa) even in cooling from 500 to 20 °C during 3.8 h.

Thus, regardless the effective influence of deformations of instantaneous plasticity and creep in 900–500 °C temperature interval, application of DW or brazing of copper (silver) braze alloys can result in assembly fracture.

Sufficiently high temperatures of DW are to be noted when considering technological variants of graphite-to-copper joining. Work [2] investigates three variants of graphite-titanium DW, namely with nickel interlayer of 10–30 µm thickness deposited on graphite by galvanic method, with nickel foil of 10 µm thickness, and directly graphite to titanium. Temperature of 850 °C was taken in welding with nickel interlayer, and that without interlayer made 1100 °C. Such high temperatures of DW do not allow using these methods in given assemblies.

Brazing allows regulating a stress level by changing temperature interval of cooling via selection of braze alloys with necessary melting temperature, providing serviceability of the assemblies under specific conditions. The calculations showed that application of low-temperature braze alloys with melting temperature up to 250 °C guarantees production of defect-free joints. For example, POS-50 braze alloy with melting temperature 209 °C provides for tensile strength equal 36 MPa, i.e. at graphite level. Taking into account lead toxicity, it is reasonable to use substitutes of tin-lead braze alloys, for example, low-temperature ones developed at the E.O. Paton Electric Welding Institute, in which lead is replaced by small amounts of silver. If graphite wetting by braze alloy requires higher temperature, than brazing is reasonable to be carried out by two-step technology with pretinning of graphite surface. Thus, graphite-to-copper brazing with further slow cooling is more practical. Time of cooling is to be calculated for specific assembly using copper creep parameters.

Conclusions

1. All constituents of stresses and deformations are significantly changed with cooling rate vari-

ation. Further holding at 500 °C changes them more.

2. Reduction of cooling rate from the point of view of development of plastic deformations is more efficient than increase of holding time after temperature reduction to 500 °C. This promotes for reduction of the level of stresses in the assembly at cooling.

3. Internal surface has the highest risk of crack formation after cooling, where in all variants, except for variant 5, the maximum tensile stresses reach graphite bending strength.

4. Variant 5 (gradual reduction of temperature from 900 to 500 °C during 6000 s), at which tensile stresses do not exceed 25 MPa, is considered the most optimum from the point of view of reduction of danger of crack formation in graphite after cooling to 500 °C.

5. Variants with quick cooling and further holding are not reasonable since large stresses on the external surface of graphite are developed at them.

6. Brazing with low-temperature lead-free braze alloys is the most practical for production of copper-graphite assemblies from low-strength graphite.

1. Ermolaev, G.V., Kvasnytsky, V.V., Kvasnytsky, V.F. et al. (2015) *Brazing of materials*: Manual. Ed. by V.F. Khorunov et al. Mykolaiv: NUK.
2. Kazakov, N.F. (1976) *Diffusion welding of materials*. Moscow: Mashinostroenie.
3. Kvasnytsky, V.V., Ermolaev, G.V., Matvienko, M.V. (2008) Influence of plastic deformation on stress-strain state in diffusion welding of dissimilar metals applicable to cylinder–cylinder and bush–bush assemblies. *Zbirnyk Nauk. Prats NUK*, **1**, 100–107.
4. Makhnenko, V.I., Kvasnytsky, V.V., Ermolaev, G.V. (2008) Stress-strain state of diffusion bonds between metals with different physical-mechanical properties. *The Paton Welding J.*, **8**, 2–6.
5. Kvasnytsky, V.V., Ermolaev, G.V., Matvienko, M.V. (2009) Influence of strength and creep resistance on residual stress-strain state of metal-ceramic joints. *Zbirnyk Nauk. Prats NUK*, **3**, 83–92.
6. Kvasnytsky, V.V., Ermolaev, G.V., Matvienko, M.V. (2008) Influence of geometry of dissimilar materials parts on stress-strain state in diffusion welding. *Ibid.*, **5**, 42–46.
7. Kvasnytsky, V.V., Matvienko, M.V., Ermolaev, G.V. (2009) Influence of the ratio of dimensions of cylindrical parts from dissimilar materials on their stress-strain state in diffusion welding. *The Paton Welding J.*, **8**, 17–20.

Received 21.07.2015